Phase Transitions in $(CH_3)_4NMnCl_3$ (TMMC) and Related Compounds*

P. S. Peercy, B. Morosin, and G. A. Samara
Sandia Laboratories, Albuquerque, New Mexico 87115
(Received 4 May 1973)

The order-disorder phase transitions in the linear chain compounds $(CH_3)_4NMnCl_3$ (TMMC), $(CH_3)_4NNiCl_3$ (TMNC), and $(CH_3)_4NCdCl_3$ (TMCC) were investigated using the complementary techniques of x-ray diffraction, Raman scattering, and low-frequency dielectric-constant measurements. The three compounds have isomorphous hexagonal structures (space group $P6_3/m$) at room temperature and transform to monoclinic structures at low temperature. The transitions occur at 126 (TMMC), 171 (TMNC), and 118 °K (TMCC); in their low-temperature phases, TMMC and TMNC are isomorphous with space group $P2_1/a$, while TMCC belongs to space group $P2_1/m$. The nature of the dielectric-constant anomaly at the transition coupled with the fact that the unit cell doubles on cooling through the transition suggest that TMMC and TMNC may be antiferroelectric in their low-temperature phase while TMCC is not. Measurements of the pressure dependence of the dielectric constants further suggest that the low-temperature phase of TMMC changes from TMNC-like to TMCC-like at pressures greater than ~ 2 kbar. This pressure-induced phase transition is believed to be a consequence of the highly anisotropic compressibility of TMCC and the attendant increase in c/a with pressure. The large a-axis compressibilities are also responsible for the observed large increase of the transition temperatures T_t with pressure. Pressure reduces the separation between the linear chains, thus hindering the motion of the tetramethylammonium ions and causing T_t to increase.

I. INTRODUCTION

Tetramethylammonium manganese chloride, $(CH_3)_4NMnCl_3$ (TMMC), has been shown to be a linear magnetic system for temperatures above 1 °K, and neutron scattering experiments[1] demonstrated that its behavior is that of an ideal one-dimensional antiferromagnet. Because of this linear magnetic behavior, TMMC has been the subject of several recent experimental investigations. The crystal structure was determined originally by Morosin and Graeber[2] who found that the crystal contains infinite linear chains of face-shared $MnCl_6$ octahedra ($\cdots$ Mn-Cl_3-Mn-$Cl_3\cdots$) separated by tetramethylammonium (TM) ions. Measurements of the magnetic susceptibility[3] demonstrated the one-dimensional magnetic behavior inferred from the infinite-linear-chain structure, and it was found from neutron scattering measurements[1] that the system obeyed Fisher's[4] theory for a classical Heisenberg linear chain. Further measurements of the magnetic properties of TMMC have been made using EPR[5] and NMR[6,7] techniques.

In addition to the interesting magnetic properties of this crystal, TMMC[1,8] and the isomorphous compounds $(CH_3)_4NCdCl_3$ (TMCC)[9] and $(CH_3)_4NNiCl_3$ (TMNC) exhibit structural phase transitions which are of interest from a lattice-dynamical point of view. A transition was first observed in TMMC where it was investigated by neutron,[1] x-ray,[8] and Raman scattering[8] measurements. The Raman scattering measurements indicated that the transition is of the order-disorder type, similar to that in NH_4Cl[10] and NH_4Br,[11] driven by the ordering of the TM ions. At room temperature the TM ions are orientationally disordered, and, upon cooling, the crystals undergo phase transitions in which the TM ions order producing an attendant change in the symmetry of the unit cell. While this order-disorder transition occurs at relatively high temperatures (~ 126 °K for TMMC), Mangum and Utton[7] recently reported evidence for another transition at low temperatures ($T \sim 45$ °K) in TMMC which also involves reorientation of the TM ions. Their conclusions were based on changes in the NMR spectrum which occurred in the temperature range 40–50 °K.

We have made detailed measurements of the temperature dependence of the crystal structure and phonon spectra of TMMC, TMNC, and TMCC using x-ray and Raman scattering techniques. In addition, the temperature and pressure dependences of the low-frequency dielectric constants were measured. These are the first measurements of the dielectric properties for these materials and reveal important differences in the dielectric behavior of the different crystals. The purpose of this paper is to present and discuss the results of these three types of measurements. The experimental arrangements are given in Sec. II and the results are presented and discussed in Sec. III. Section IV contains a brief summary and conclusions.

II. EXPERIMENTAL CONSIDERATIONS

A. Samples

Single crystals were grown by slow evaporation of saturated solutions prepared with stoichiometric amounts of $N(CH_3)_4Cl$ and the appropriate metal chloride. After preparation such solutions were

slightly acidified with HCl if the metal hydroxide appeared to form. In the case of TMCC, cooling a hot saturated solution yielded very small single crystals. To obtain larger crystals, the solutions were allowed to evaporate slowly. The resulting crystals of TMCC and TMNC were ~1–2 mm on a side whereas crystals of TMMC as large as 10–15 mm on a side were obtained, although most of the larger crystals contained appreciable imperfections

B. X-ray Measurements

Experimental details of the room-temperature single-crystal x-ray structure determinations were given previously.[2,12] Similar techniques were used for room-temperature measurements in the present study. Single crystals were mounted to allow investigation along various symmetry directions (usually [0001], [11$\bar{2}$0], or [10$\bar{1}$0]) and film and/or Polaroid Weissenberg and precession photographs were taken both at room temperature and low temperature ($\gtrsim$100 °K). The transitions were found to be reversible by several measurements on more than one specimen of each type. No single-domain specimens were obtained at low temperature, however, as twinning occurred in all cases; furthermore, the domain distribution did not vary on recycling nor from specimen to specimen. This behavior has been observed in other phase transitions.[13]

For the low-temperature photography, the samples were cooled with flowing N_2 gas. The temperature was monitored by two thermocouples, one on the source side of the N_2 stream and the other mounted on the sample holder. The absolute temperature accuracy was ±5°K.

For measurements on TMMC between 5 and 100 °K, a cryostat for single-crystal x-ray studies was used. The temperature was measured with a calibrated Ge resistance thermometer attached to the copper sample block. Cu$K\alpha$ radiation was used to measure both the 2θ value and intensity.

To measure the axial compressibilities (TMMC only), the sample was mounted in a beryllium high-pressure cell, and dehydrated kerosene was used as the pressure fluid. Details of the pressure apparatus have been given elsewhere.[14]

C. Raman Scattering Measurements

Both argon and krypton lasers were used to obtain the Raman spectra. Different excitation frequencies were used for the different materials to avoid the strong absorption bands of the particular sample. For TMMC and TMCC, the data were obtained with the 4880-Å line of argon and checked with the 4579-Å line. TMNC is strongly absorbing in the blue region of the spectrum and the data were obtained with the 6471-Å line of krypton and checked with the 6764-Å line.

In all measurements the samples used were polished single crystals; owing to the small dimensions (~1 mm on a side) of the TMNC and TMCC, detailed measurements were not made for the low-frequency region of the spectra because of the large elastically scattered intensity. This low-frequency region of the spectra, which contains an overdamped rotational mode of the TM ions, was investigated in detail for TMMC, where large crystals (~3–5 mm on a side) of good optical quality were available.

The data were taken on a right-angle scattering geometry with incident power of < 200 mW. The scattered light was analyzed with a double-grating spectrometer and detected with a cooled photomultiplier. Signals from the photomultiplier were measured using photon-counting electronics. For temperatures below room temperature, the samples were mounted in a variable-temperature Dewar and cooled with the boil off from liquid helium. The temperature was stabilized to ±0.5 °K and monitored at the sample block using either Ge or Pt resistance thermometers. Absolute temperature measurement was much poorer than this, however, due to sample heating from the previously mentioned absorption.

D. Dielectric Measurements

Owing to the lack of suitably large single crystals, the static dielectric-constant measurements were made on polycrystalline specimens of essentially theoretical density prepared by grinding the small crystals and fusing the powder in a die at pressures of ~10 kbar. The resulting specimen discs had areas of 0.71 cm^2 and thicknesses ranging from 0.06 to 0.10 cm. Air-drying silver-paint electrodes were applied to the large faces and proved quite satisfactory; the electrodes adhered well and gave reproducible and reversible results.

The dielectric constants were determined from capacitance measurements at either 1 or 100 kHz using General Radio Model Nos. 1615-A and 1673-A capacitance bridges. Shielded electrical leads were used thoughout and capacitances were measured to a precision better than ±0.2%. The absolute accuracy of the calculated dielectric constants is not this good, however, since specimen capacitances were typically ~2 pF and guard-ring electrodes were not used. This is of no concern here since we are primarily interested in the relative changes and the behavior of the dielectric constant with temperature and pressure, especially near the phase transitions.

The specimens were held in a beryllium copper (Beryllco 25 hardened to RC39-41) cell which also served as the high-pressure cell. Helium gas was used as the pressure medium. The temperature and pressure measurements were fairly standard

TABLE I. Comparison of structural parameters of TMMC, TMNC, and TMCC above and below T_t.

	Room Temperature		
	TMMC	TMNC	TMCC
a_0(Å)	9.151	9.019	9.138
c_0(Å)	6.494	6.109	6.723
c_0/a_0	0.710	0.677	0.736
M-Cl(Å)	2.560	2.408	2.644
Cl-M-Cl′ (chain)	95.91°	95.95°	96.09°
Cl-M-Cl′ (plane)	84.09°	84.05°	83.91°
T_t(°K)	126.5	171.0	118.5
	Low Temperature		
	TMMC (~105°K)	TMNC (~100°K)	TMCC (~115°K)
a_0(Å)	18.25	18.15	9.27
b_0(Å)	8.95	8.91	8.79
c_0(Å)	6.45	6.08	6.69
γ	120.69°	120.7°	118.6°
Space Group	$P2_1/a$	$P2_1/a$	$P2_1/m$

and similar to those described previously.[15] Temperature changes were measured to ±0.1°K using calibrated copper-constantan thermocouples, and the pressure was measured by a calibrated Heise bourdon-tube gauge to ±0.5%.

III. RESULTS AND DISCUSSION

A. Structural Properties

1. Room-Temperature Structures

At room temperature TMMC, TMNC, and TMCC have hexagonal crystal structures which are isomorphous.[2, 12, 16] The lattice constants for these crystals are given in Table I. The structure belong to the space group $P6_3/m$ with chloride ions fixed at mirror planes $\frac{1}{4}$ and $\frac{3}{4}$ along c and TM ions statistically disordered on these mirror planes (Fig. 1). Both x-ray[2, 12] and neutron scattering data[1] indicate that the TM ions are statistically disordered about the threefold axes at $\frac{1}{3}$, $\frac{2}{3}$, $\frac{1}{4}$ and $\frac{2}{3}$, $\frac{1}{3}$, $\frac{3}{4}$ and undergo significant thermal motion. Of particular interest in this structure are the infinite linear chains of metal-chloride ions ($\cdots M\text{-}Cl_3\text{-}M\text{-}Cl_3\text{-}M\cdots$) which run parallel to the c axis (such a chain is illustrated in Fig. 1). The metal ions are separated by ~3.3 Å = $\frac{1}{2}c$ along the chain axis; because of the large intervening TM ions, the interchain metal-ion separations are ~9 Å = a. For TMMC this produces magnetic linear chains which are effectively isolated from each other and results in its one-dimensional magnetic properties at low temperature.

2. Phase Transitions and Low-Temperature Strucutres

Upon cooling, these compounds undergo completely reversible hexagonal to monoclinic crystallographic phase transitions.[1, 8] The 1-bar low-temperature crystal structures of TMMC and TMNC are isomorphous while the low-temperature phase of TMCC belongs to a different monoclinic-type structure. As will be seen later (Sec. III B) the Raman scattering measurements indicate that the phase transitions are driven by the ordering of the TM ions. This ordering requires only slight shifts of the $\cdots M\text{-}Cl_3\text{-}M\text{-}Cl_3\text{-}\cdots$ chains relative to each other with the internal structure of the chains remaining essentially unchanged.

In the case of TMMC and TMNC, diffraction photographs of the low-temperature phases show splittings consistent with twinning as well as additional reflections consistent with a doubling in the length of the unit cell along one of the original hexagonal axes. The additional reflections are of the general type (h k l) (using Miller indices defined by the monoclinic lattice taking c as the unique axis) but are absent for (h k 0) when h is odd. Together with the systematic absence of odd l for (0 0 l), the data therefore indicate that this low-temperature structure belongs to the space group $P2_1/a$. The lattice constants[17] are given in Table I. In the case of TMCC, diffraction photographs of the low-temperature phase show a

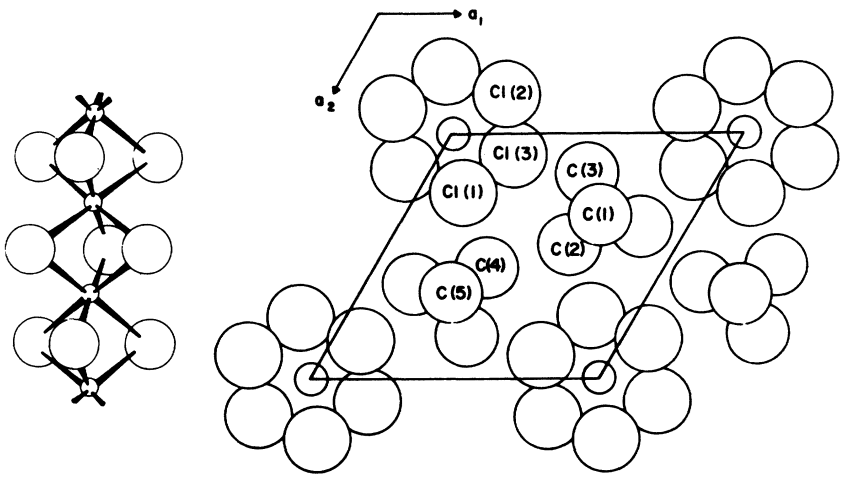

FIG. 1. Representation of the room-temperature structure of TMMC. Linear chains, shown on left-hand side, are located parallel to the c axis at the origin of the hexagonal cell. The TM ions are located on three-fold axes in an orientationally disordered manner on planes $\frac{1}{4}$ and $\frac{3}{4}$ along z.

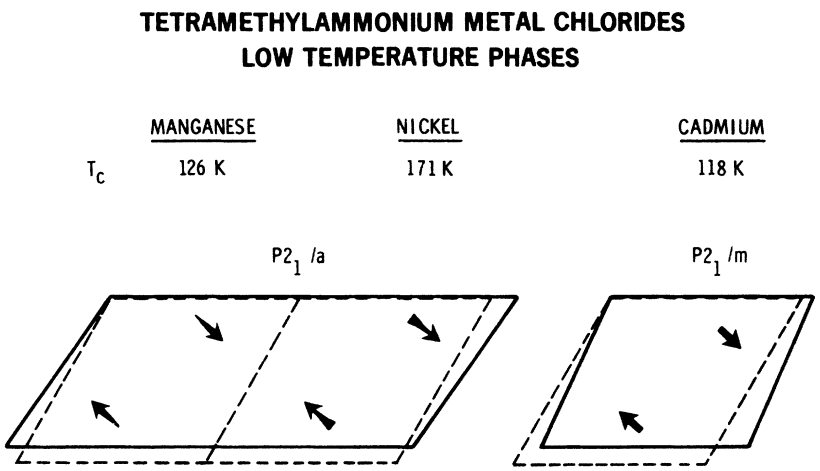

FIG. 2. Illustration of the low-temperature structure of TMMC. The dashed cell indicates the room-temperature cell; the solid lines indicate the monoclinic cell and the distortions are greatly exaggerated for illustrative purposes. The glide operation of the space group relates TM positions in a manner similar to that suggested by the arrows, in which a fat (thin) tail implies tipping towards (away) from the observer.

slightly larger distortion of the hexagonal cell than that observed for TMMC and TMNC, and the unit cell volume does not double. The Bragg intensities may be indexed consistent with a monoclinic cell of dimensions given in Table I. Although the space group $P2_1/m$ is selected, the lower symmetry noncentrosymmetric space group $P2_1$ cannot be ruled out.

Comparison of the observed intensities above and below the phase transitions suggests that the primary changes which occur at the phase transition involve the TM ions. This hypothesis is substantiated by the Raman scattering measurements (Sec. III B). When viewed along the $\cdots M\text{-}Cl_3\text{-}M\text{-}Cl_3\cdots$ chains, the projections of the two halves (along the doubled a edge) of the unit cells for TMMC and TMNC are identical due to the direction of the a-glide operation, i.e., the only differences occur with respect to the z (monoclinic) coordinates of the atoms of the TM ions. This is indicated in Fig. 2 which shows the cell edges and angles greatly exaggerated for illustrative purposes. The phase transitions leave the relative positions of the linear chains unchanged (see room-temperature structure shown in Fig. 1) while causing the TM ions to order. The ordering of the TM ions is illustrated schematically in Fig. 2 by arrows near locations of TM ions in the room-temperature structure (on three-fold axes).

Comparison of the room-temperature angles given in Table I indicates that the $\cdots M\text{-}Cl_3\text{-}M\text{-}Cl_3\cdots$ chains are very similar in the different compounds. The primary difference is the metal-chlorine separation due to the different radii of the metal ions, and this is reflected in the differences in the lengths of the c axes. The TM ions sit in the voids between the chains. Determination of the exact orientation of the TM ions as well as the exact low-temperature chain parameters would require an involved series of measurements (because of twinning in the low-temperature phase) which were considered beyond the scope of the present study. (Previous studies on other materials suggest interchain angles change very little over a 200 °K temperature difference; one can note the c-axis lengths change less than 1% or ~5 times the estimated error in the metal-chloride-ion separation.)[18]

To investigate the suggestion by Mangum and Utton[7] that TMMC has a structural phase transition near 40 °K, the intensity and 2θ value for a series of Bragg reflections were measured be-

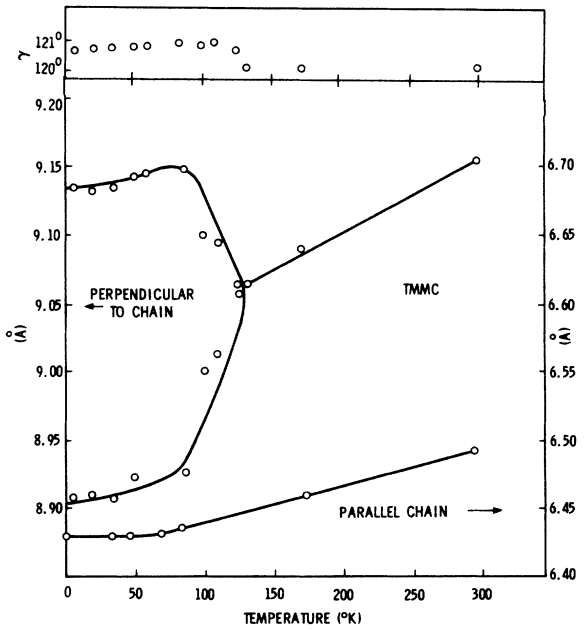

FIG. 3. Temperature dependence of the lattice constants of TMMC above and below the phase transition. In the curves perpendicular to the chains (monoclinic phase) the upper branch is $\frac{1}{2}a$ and the lower branch is b. The temperature dependence of the angle γ is also shown.

tween 4 °K and 125 °K using a crystal specimen which, though a single crystal at room temperature, showed the typical twinning behavior below the phase transition. In particular, the (004), (008), (16 00), and (080) (monoclinic indices) yield lattice constants as a function of temperature (Fig. 3) which are in good agreement with the value of Hutchings *et al.*[1] The intensities for the above indices, as well as the (401) [(021) and (4$\bar{2}$1) superimpose], (601) [(03$\bar{1}$) and (6$\bar{3}$1) superimpose], (204) [(014) and (2$\bar{1}$4) superimpose], (510), and (140) reflections, were measured as a function of temperature.

The (510) and (140) reflections are observed only for the monoclinic phase and yield information about the ordering of the TM ions. The intensity of the (140) reflection gradually increases with decreasing temperature from 125 to ~ 60 °K. From 60 to 5 °K the intensity remains constant. The intensity for the (510) reflection initially increases more rapidly with decreasing temperature than the (140) and levels off by ~ 40 °K. Near 35 °K it exhibits a small (~ 10%) but abrupt intensity increase and the intensity continues to increase slightly from 35 to 5 °K. Only the (510) reflection exhibited an abrupt intensity change in this temperature region.

We interpret the gradual increase in intensity as the temperature decreases from 125 °K to be due to the decrease in the thermal motion of the TM ions and the rather abrupt increase in the (510) intensity at ~ 35 °K to result from the freezing out of the rotational motion of the methyl (CH_3) groups of the TM ions. This would increase the intensity without altering the over-all orientation of the TM ions. The fact that none of the other measured reflections exhibited a statistically significant change in intensity near 35 °K suggests that the atoms which contribute to the scattering have not altered their positions nor the degree of their thermal motion in the lattice. This conclusion disagrees with the interpretation given by Mangum and Utton[7] for the temperature dependence of the NMR spectra in TMMC.

3. *Axial Compressibilities of* TMMC *at Room Temperature*

The axial compressibilities of TMMC were measured at room temperature. Intuitively, one would expect the compressibility normal to the linear chains (*a* axis) to be appreciably larger than the compressibility along the chain (*c* axis), since the electrostatic forces between the TM ions and the linear chains encountered along the *a* axis are weak compared to the forces along the *c* axis of the crystal which has the chemically bonded $\cdots M\text{-}Cl_3\text{-}M\text{-}Cl_3\cdots$ chains. That this is the case is evident from Fig. 4 which shows the pressure dependences of the reduced lattice constants. The room-temperature values for the axial compressibilities are $\kappa_a = -(\partial \ln a/\partial P)_T = 20.0\times10^{-4}$ kbar^{-1} and $\kappa_c = -(\partial \ln c/\partial P)_T = 4.2\times10^{-4}$ kbar^{-1}. At room temperature the c/a ratio (Table I) is 0.677 for TMNC, 0.710 for TMMC, and 0.736 for TMCC. Since $\kappa_a > \kappa_c$ for TMMC, the effect of pressure is to increase the c/a ratio so that at high pressure the structure of TMMC becomes more similar to TMCC. The implications of this will be discussed below in relation to a new pressure-induced phase transition in TMMC (Sec. III C).

B. Raman Scattering Measurements

In Sec. III A we noted that the room-temperature phase of TMMC, TMNC, and TMCC belong to the space group $P6_3/m$ with two formula weights per unit cell and that the crystals have only one linear chain per unit cell. Thus the lattice vibrations of these compounds are expected to be very similar with the major differences produced by the differences in the mass of the metal ions and the atomic separations. Since the crystals are composed of strongly bonded TM ions which are weakly bound to the $\cdots M\text{-}Cl_3\text{-}M\text{-}Cl_3\cdots$ chains, the vibration spectra can conveniently be separated into internal modes of the TM ions and the lattice modes which result when the TM ions are considered as rigid units in the crystals. The lattice modes will also include the librational modes of the TM ions.

The irreducible representation for the optic modes external to the TM ions is[19]

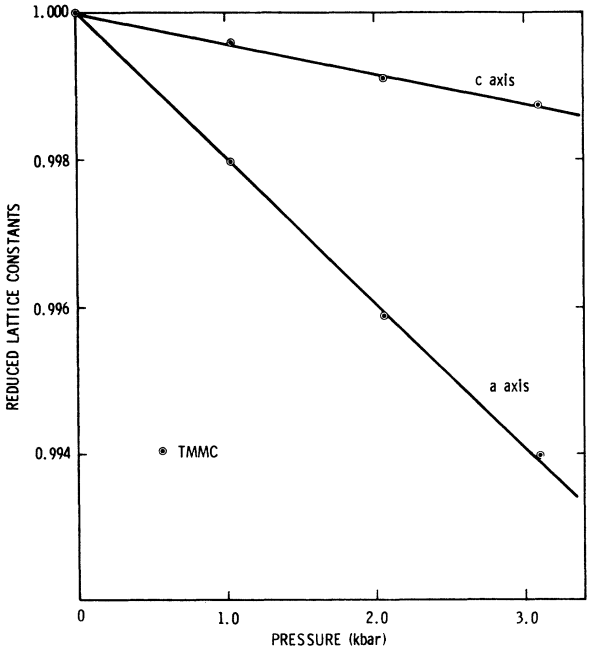

FIG. 4. Pressure dependence of the reduced lattice constants of TMMC.

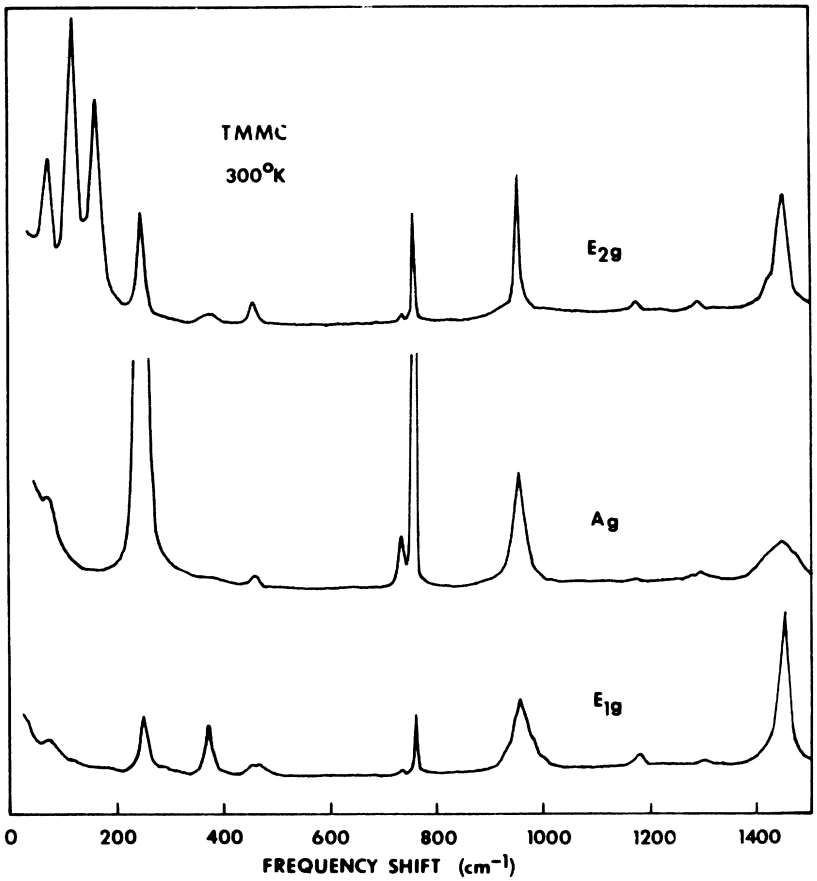

FIG. 5. Room-temperature spectra of TMMC from 0 to 1500 cm^{-1} for three Raman-active symmetries.

$$\Gamma_{ext} = 3A_g + 2A_u + 2B_g + 4B_u + 2E_{1g} + 3E_{1u} + 3E_{2g} + 3E_{2u}. \quad (1)$$

Modes of symmetry A_g, E_{1g}, and E_{2g} are Raman active. The origin of the Raman-active modes can be identified more precisely: The three modes of A_g symmetry include a TM librational mode, a chain librational mode and an internal mode of the chain; E_{1g} contains a librational mode of the chain and a chain internal mode, while E_{1g} has two chain internal modes and a relative translation of the two sublattices.

The nonzero components of the polarizability tensor for the Raman-active modes are $(xx+yy, zz)$ for A_g, (xz, yz) for E_{1g}, and $(xx-yy, xy)$ for E_{2g}. Traces taken at room temperature showing the different symmetry modes for TMMC from 0–1500 cm^{-1} are shown in Fig. 5. The spectra for the high-temperature phases of TMNC and TMCC are similar to those for TMMC and are not shown. The positions and assignments of these modes are compared in Table II.

It should also be noted that the three compounds exhibit the internal modes of the TM ions. These occur at higher frequencies and are quite similar in the three compounds and will not be discussed here, except to note that their positions correspond closely to the positions observed for the free TM ion.[20]

Of more interest are the changes accompanying the phase transitions. It was previously noted that the low-temperature Raman spectra for the external modes were markedly different for TMMC and TMCC[8] because of the different crystal symmetries. However, the internal modes of the linear chains are unaffected by the phase transtion, indicating that these units are unchanged by the transition even though the symmetry has been re-

TABLE II. Comparison of the Raman-active lattice modes in the room temperature phases of TMMC, TMNC, and TMCC.

Symmetry	Position (cm^{-1}) TMMC	TMNC	TMCC	Probable assignment
A_g	252	269	248	Chain (internal)
E_{2g}	173	192	164	Chain (internal)
E_{2g}	122	134	118	Chain (internal)
E_{2g}	83	93	74	Translation
E_{1g}	118	130	not obs.	TM (rotation)
A_g	81[a]	89	80[a]	Chain (rotation)

[a]Value at 230 °K.

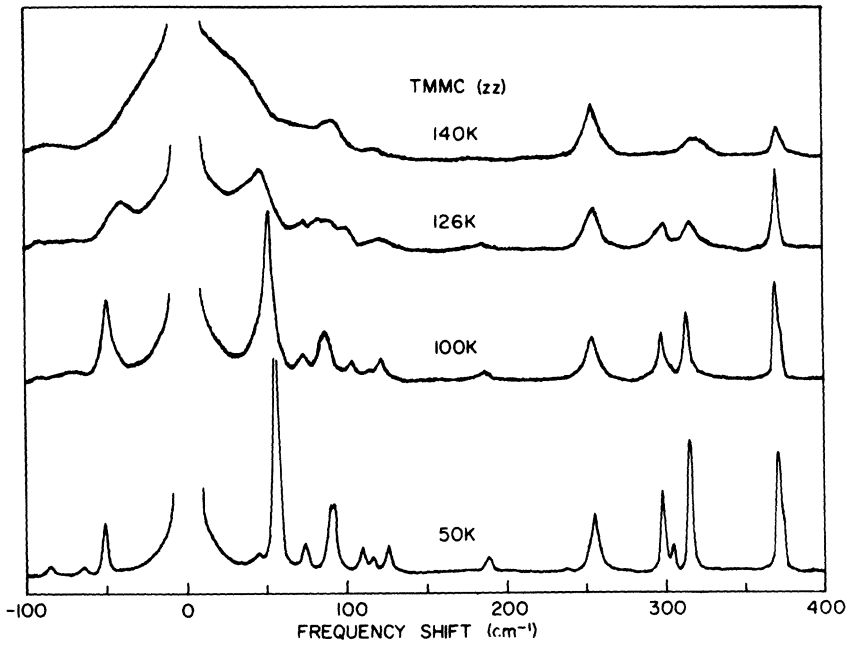

FIG. 6. Region of the A_g Raman spectra for TMMC from -100 to 400 cm^{-1} showing the temperature dependence of the rotational mode.

duced. We will not attempt to give a detailed assignment of the symmetries of the modes in the low-temperature phases here but rather wish to concentrate on the rotational modes of the TM ions.

Figure 6 shows the region of the A_g spectra of TMMC which contains the TM librational mode for various temperatures above and below the transition temperature T_t. At $T > T_t$, the mode is over-

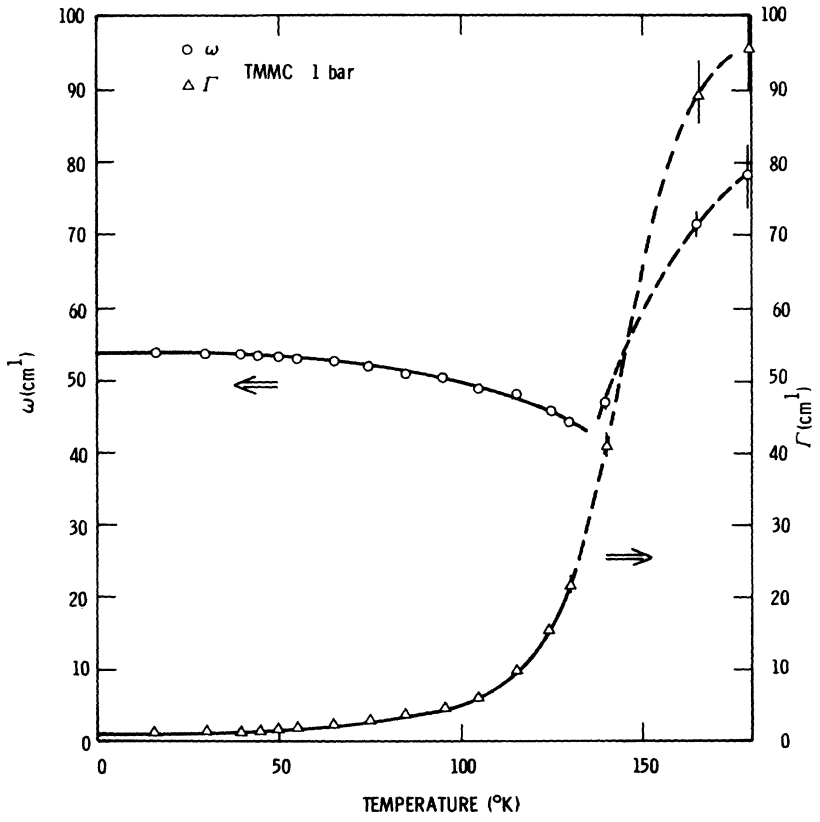

FIG. 7. Temperature dependences of the frequency and linewidth of the librational mode in TMMC.

damped and appears as a broad shoulder on the laser line. As the temperature decreases, the damping decreases and at T_t the mode becomes underdamped. On further decrease in temperature, the damping of the now well-resolved mode continues to decrease until the linewidth becomes resolution limited. Below T_t the frequency exhibits a substantial temperature dependence, increasing from 45 cm^{-1} at T_t to 53 cm^{-1} at 2 °K. The temperature dependence of the damping and frequency are shown in Fig. 7.

To evaluate the frequency ω and damping Γ for $T > T_t$, an assumption must be made concerning the nature of the librational motion. If there are no long-range interactions between the TM ions, the spectra would represent a single-particle-like response of the system; however, long-range interactions would produce an overdamped propagating mode. As we shall see below, if the excitation is assumed to be that of an overdamped harmonic oscillator, reasonable behavior is obtained for ω and Γ, at least for the temperature range near T_t.

The power spectrum $S(\omega)$ of the scattered light is

$$S(\omega) \propto \mathrm{Im}\chi(\omega)\ [\bar{n}(\omega)+1], \tag{2}$$

where $\bar{n}(\omega) = [e^{\hbar\omega/kT} - 1]^{-1}$ and $\chi(\omega)$ is the complex susceptibility. For an harmonic oscillator of a single frequency ω_0 and frequency-independent damping Γ_0, the imaginary part of $\chi(\omega)$ is of the form

$$\mathrm{Im}\chi(\omega) = 2\omega\Gamma_0\omega_0^2\chi(0)/[(\omega_0^2 - \omega^2)^2 + 4\omega^2\Gamma_0^2], \tag{3}$$

where $\chi(0)$ is the static susceptibility. ω_0 and Γ_0 are evaluated by performing a least-squares-fit to the data for the spectral region from -100 to 100 cm^{-1}. The results are shown in Fig. 7. It should be noted that for $\Gamma_0 > \omega_0$ the response is relaxationlike with a relaxation rate of ω_0^2/Γ_0, and independent values of ω_0 and Γ_0 are no longer very meaningful.

If the TM reorientation is thermally activated, the damping would be expected to exhibit a temperature dependence of the form[10,11]

$$\Gamma(T) = Ke^{-E/kT}, \tag{4}$$

where E represents a barrier energy separating the different positions. Equation (5) assumes a single barrier, i.e., only one type of reorientation. This assumption is inadequate to explain the temperature dependence for the linewidth of the vibrational mode in TMMC. A similar complicated temperature dependence is observed in the linewidth of the librational mode in $NaNO_3$ near the order-disorder transition.[21] In $NaNO_3$ the deviation of the linewidth $\Gamma(T)$ from the behavior predicted by Eq. (4) is attributed to the existence of two distinct potential barriers and the data are found to agree with a more complex equation for $\Gamma(T)$ based on the known structural properties of the crystal.

Plausibility arguments can be made for the existence of more than one potential barrier in TMMC based on our knowledge of the structural changes which occur at the phase transition (Sec. III A). At low temperature ($T < T_t$) the TM ions are ordered and undergo librational motion about their ordered positions. At a high temperature ($T > T_t$) the TM ions exhibit both statistical (deviations about a high-symmetry axis) and positional (general orientation, e.g., "up" or "down" of the high-symmetry axis) disorder. In view of this information, we attempted to fit the temperature dependence of $\Gamma(T)$ to the expression derived by Fontaine[21] for the simpler $NaNO_3$ case. The fit was not good. It therefore appears that a model based on the detailed structural properties of TMMC is required to explain the temperature dependence of the linewidth of this mode.

C. Dielectric Constants and the Pressure Dependence of the Transition Temperature

It has previously been established that the low-temperature phase of TMMC is different from that of TMCC.[8] Furthermore, the present work shows that the low-temperature phases of TMNC and TMMC are identical. A very sensitive means of

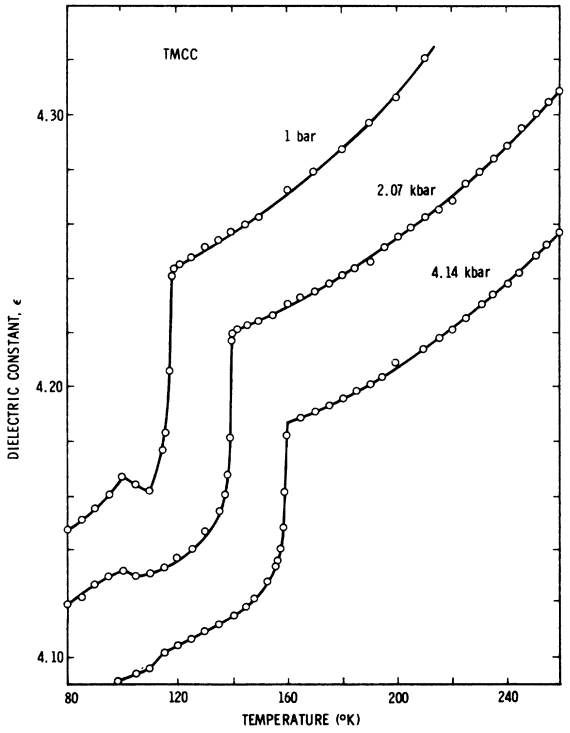

FIG. 8. Temperature dependence of the dielectric constant of TMCC for various pressures.

studying the detailed features of phase transitions in dielectrics is to measure the static-dielectric constant through the transitions.[22] The present measurements of the effects of temperature and pressure on the dielectric constants of these materials were motivated largely by the desire to study the nature of the transitions and the effects of pressure on the transition temperatures. The dielectric data are, of course, also of interest in their own right as we shall observe. We shall also see that the dielectric results emphasize the differences in the low-temperature structures and the character of the transitions. The measurements consisted of the variation of the static dielectric constant ϵ (an average bulk value since the specimens were polycrystalline) with temperature at atmospheric pressure as well as elevated pressures. All of the observed effects are completely reversible, and the results are shown in Figs. 8–11. We now consider the data for each compound:

1. TMCC

The results on TMCC are shown in Fig. 8. In the high-temperature phase ϵ decreases monotonically with decreasing temperature at atmospheric pressure as well as with increasing pressure at constant temperature—behavior characteristic of normal ionic crystals. The decrease in ϵ results from the decrease of the ionic polarizability with decreasing volume (the crystal gets stiffer). The effect due to change in density is opposite in sign from the measured effect and plays a lesser role. On further cooling a phase transition, marked by a sharp decrease of ~ 2% in ϵ, is observed at 118.5 °K. This drop in ϵ at the transition is quite sharp considering the fact that the specimen is fused powder. In the low-temperature phase ϵ again decreases monotonically with decreasing temperature and increasing pressure. A small anomaly in ϵ is observed at ~100 °K. Its origin is not known. It may be spurious and will not be considered further. The transition temperature T_t is very pressure dependent and increases linearly with pressure over the 4-kbar range investigated with a slope $dT_t/dP = (10.25 \pm 0.40)$° K/kbar (see Fig. 11).

2. TMNC

The behavior of TMNC shown in Fig. 9 is drastically different than that of TMCC (cf. Fig. 8). In the high-temperature phase, ϵ increases with decreasing temperature and $|d\epsilon/dT|$ is larger than that for TMCC. At the transition, $\epsilon(T)$ is rounded and the decrease in ϵ on the low-temperature side of the transition is very gradual, extending over many degrees. The magnitude of the decrease in ϵ at the transition is ~20%, which is approximately an order of magnitude larger than the decrease for TMCC. The magnitude of the change in ϵ on going through the transition decreases with increasing pressure. For $T \ll T_t$, ϵ decreases with temperature in a "normal" manner.

In the high-temperature phase the $\epsilon(T)$ response obeys a Curie law of the form $\epsilon \propto T^{-1}$ fairly well. This feature, along with the nature of the $\epsilon(T)$ behavior near the transition are characteristic of the dielectric response generally observed for materials exhibiting ferroelectric or antiferroelectric transitions. Coupling these observations with the fact that the unit cell doubles on cooling through the transition suggests that the low-temperature phase of TMNC may be antiferroelectric. The gradual increase exhibited by ϵ as $T \to T_t$ from below is also characteristic of onset of disorder. Such behavior is observed for substances with second-order (or nearly second-order) phase transitions.

At 1 bar $T_t = (171.0 \pm 1.0)$° K, where T_t is taken as the temperature corresponding to ϵ_{max}; T_t increases linearly with pressure (Fig. 11) with a slope $dT_t/dP = (6.4 \pm 0.5)$° K/kbar. We note that this slope is approximately one-half of that for TMCC.

3. TMMC

Some of the results for TMMC are shown in Fig. 10. One of the more obvious features of these data is the qualitative change in the $\epsilon(T)$ response in the transition region with increasing pressure. These results, observed on sample *A*, were checked on a completely different sample (sample *B*, prepared from a different crystal growth) to ascertain if the features were intrinsic; the results

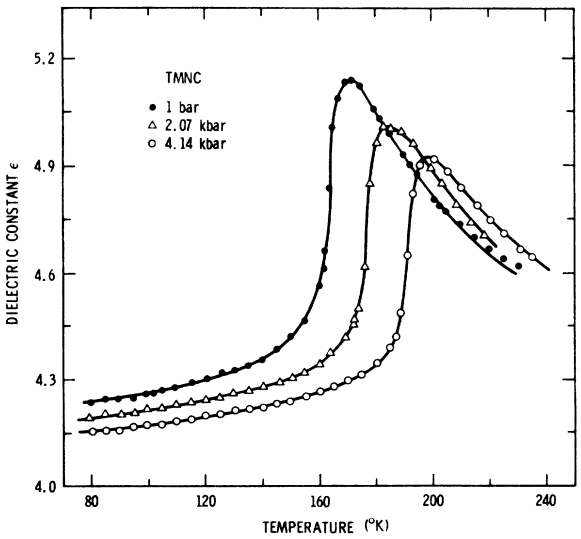

FIG. 9. Temperature dependence of the dielectric constant of TMNC for various pressures.

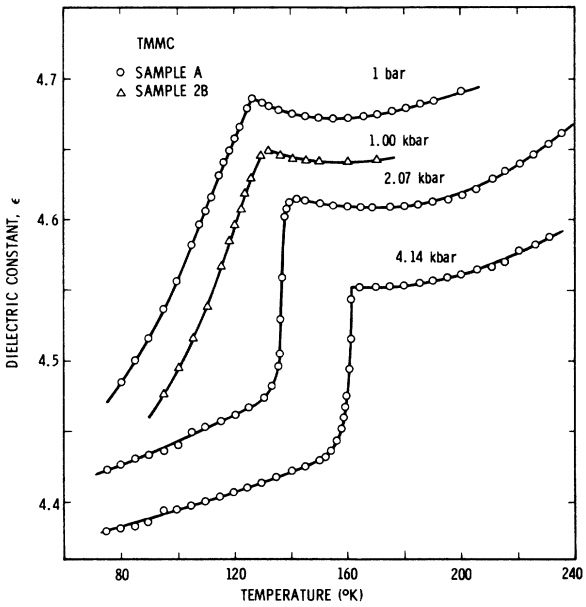

FIG. 10. Temperature dependence of the dielectric constant of TMMC for various pressures.

on sample B were in excellent agreement with those on sample A and only the 1-kbar isobar is shown in Fig. 10.

The $\epsilon(T)$ responses for the 1-bar and 1.0-kbar isobars for TMMC are qualitatively similar—both in shape and somewhat in magnitude of the changes—to the TMNC isobars shown in Fig. 9. On the other hand, the results for the 2.07- and 4.14-kbar isobars are very similar in shape and magnitude to those for TMCC shown in Fig. 8. These results suggest that at pressures $>\sim 2$ kbar the low-temperature phase of TMMC changes from a TMNC-like structure to a TMCC-like structure, i.e., there is a pressure-induced transition. Further support for this hypothesis is given by the pressure dependence of T_t for TMMC shown in Fig. 11. At 1 bar, $T_t = (126.5 \pm 1)°\mathrm{K}$. Up to ~ 2 kbar T_t increases linearly with pressure with a slope $dT_t/dP = (5.4 \pm 0.1)°\mathrm{K/kbar}$ which is comparable to that for TMNC. At ~ 2 kbar the slope changes discontinuously, and from 2–4 kbar, $dT_t/dP = (11.5 \pm 0.4)°\mathrm{K/kbar}$ which is comparable to that for TMCC. The break in the $T_t(P)$ slope in the T-P plane indicates the existence of another phase line as indicated schematically by the dotted line in Fig. 11. In fact, measurements below $\sim 130°\mathrm{K}$ have shown the existence of one or more pressure-induced phases.[23] Detailed measurements of 1 bar over the temperature range from 4 °K to T_t, however, show no anomaly in ϵ.

IV. CONCLUDING COMMENTS

The x-ray and Raman scattering results have shown that the structural transitions in the three isomorphs are of the order-disorder type. Above T_t the TM ions are orientationally disordered; below T_t they become ordered. The situation is qualitatively similar to that in the ammonium halides. The large increase in T_t with pressure is what one would intuitively expect. The crystals structures are composed of strongly-bonded negatively-charged linear chains which are widely separated (~ 9 Å) by the positively charged TM ions. The compressibility normal to the chains ($\kappa_\perp$) should therefore be much greater than that along the chains ($\kappa_\parallel$). Measurements on TMMC yield $\kappa_\perp/\kappa_\parallel \sim 5$ in agreement with this hypothesis. Thus the primary effect of pressure is to reduce the separation between the linear chains and this hinders the motion of the TM ions and causes T_t to increase. Similar behavior is observed for a large variety of different crystals which exhibit order-disorder transitions of this type. Examples range from the ammonium halides[24] to ferroelectrics like triglycine sulfate.[25]

In addition to measurements of the 126 °K transition in TMMC, detailed measurements were made in the region from 30 to 60 °K to investigate the "transition" reported by Mangum and Utton.[7] No anomaly was observed in either ϵ or in the lattice parameters. Only small changes were observed in the scattered x-ray intensity; similarly, changes were observed in the Raman scattering intensity

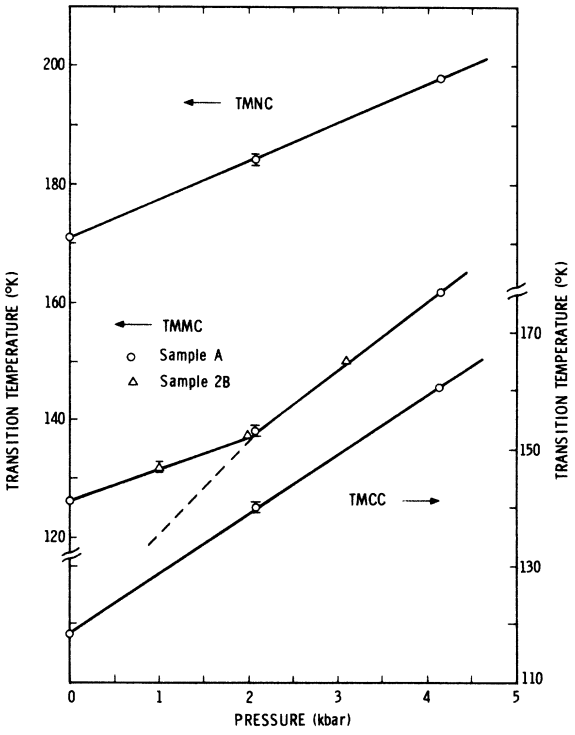

FIG. 11. Pressure dependence of the transition temperatures for TMMC, TMNC, and TMCC.

from the TM rotational mode. The x-ray intensity changes are attributed to changes in the thermal motion and not to reorientation of the TM ions. The changes in the Raman cross section are attributed to the change in the magnitude of the (zz) component of the polarizability tensor rather than to a change in the unit-cell symmetry. The results of our measurements for $T \lesssim 60\,^{\circ}\mathrm{K}$ can therefore be interpreted in terms of a "freezing out" of the rotational motion of the methyl ions without invoking a structural transition.

ACKNOWLEDGMENTS

The authors wish to acknowledge the expert technical assistance of J. D. Kluck, R. A. Trudo, and B. E. Hammons in performing most of the measurements.

---

*Work supported by the U. S. Atomic Energy Commission.

[1]M. T. Hutchings, G. Shirane, R. J. Birgeneau, and S. R. Holt, Phys. Rev. B **5**, 1999 (1972).

[2]B. Morosin and E. J. Graeber, Acta Crystallogr. **23**, 766 (1967).

[3]R. Dingle, M. E. Lines, and S. L. Holt, Phys. Rev. **187**, 643 (1969).

[4]M. E. Fisher, Am. J. Phys. **32**, 343 (1964).

[5]R. E. Dietz, F. R. Merritt, R. Dingle, D. Hone, B. G. Silbernagel, and P. M. Richards, Phys. Rev. Lett. **26**, 1186 (1971).

[6]P. M. Richards, Phys. Rev. Lett. **28**, 1646 (1972).

[7]B. W. Mangum and D. B. Utton, Phys. Rev. B **6**, 2790 (1972).

[8]P. S. Peercy and B. Morosin, Phys. Lett. A **36**, 409 (1971).

[9]P. S. Peercy and B. Morosin, Opt. Commun. **4**, 94 (1971).

[10]See, e.g., L. Rimai, T. Cole, and J. Parsons, in *Light Scattering Spectra of Solids*, edited by G. B. Wright (Springer, Berlin, 1969), p. 665.

[11]See, e.g., C. H. Wang and P. A. Fleury, in Ref. 10, p. 651.

[12]B. Morosin, Acta Crystallogr. B **28**, 2303 (1972).

[13]See, e.g., B. Morosin and A. Narath, J. Chem. Phys. **40**, 1958 (1964).

[14]P. S. Peercy and B. Morosin, Phys. Rev. B 7, 2779 (1973).

[15]G. A. Samara and P. S. Peercy, Phys. Rev. B **7**, 1131 (1973).

[16]G. D. Stucky, Acta Crystallogr. B **24**, 330 (1968).

[17]In this paper we have employed the monoclinic cell most similar to the hexagonal cell, labeling the unique symmetry direction as the c axis rather than the more commonly used (and preferred) b axis. Furthermore, as indicated in Ref. 8, the crystallographic preferred monoclinic cell usually is selected with the unique angle nearest to 90°; this would require changing the space group for TMMC to $P2_1/n$ with $a_0 \simeq 15.8$ Å, $b_0 = 6.45$ Å, $c_0 = 8.95$ Å, and $\beta \simeq 90.1\,^{\circ}$.

[18]B. Morosin, J. Chem. Phys. **44**, 252 (1966).

[19]D. M. Adams and R. R. Smardzewski, Inorg. Chem. **10**, 1127 (1971).

[20]J. T. Edsall, J. Chem. Phys. **5**, 223 (1937).

[21]D. Fontaine, C.R. Acad. Sci. B **271**, 476 (1970).

[22]G. A. Samara and W. L. Chrisman, in *Accurate Characterization of the High Pressure Environment*, edited by E. C. Lloyd, Nat. Bur. Stds. Spec. Publ. No. 326 (U. S. GPO, Washington, D. C., 1971), p. 243.

[23]G. A. Samara, B. Morosin, and P. S. Peercy, Solid State Commun. (to be published).

[24]See, e.g., C. W. Garland and R. A. Young, J. Chem. Phys. **49**, 5282 (1968).

[25]G. A. Samara, in *Advances in High Pressure Research*, edited by R. S. Bradley (Academic, New York, 1969), Vol. 3, Chap. 3.